

A Density Difference Based Analysis of Orbital-Dependent Exchange-Correlation Functionals

I. Grabowski,¹ A. M. Teale,² E. Fabiano,³ S. Śmiga,¹ A. Buksztel,¹ and F. Della Sala^{3,4}

¹*Institute of Physics, Faculty of Physics, Astronomy and Informatics,
Nicolaus Copernicus University, Grudziadzka 5, 87-100 Torun, Poland*

²*School of Chemistry, University of Nottingham, University Park, Nottingham, NG7 2RD, UK.*

³*National Nanotechnology Laboratory, Istituto Nanoscienze-CNR, Via per Arnesano, I-73100 Lecce, Italy*

⁴*Istituto Italiano di Tecnologia (IIT), Center for Biomolecular Nanotechnologies, Via Barsanti, I-73010 Arnesano, Italy*

We present a density difference based analysis for a range of orbital-dependent Kohn-Sham functionals. Results for atoms, some members of the neon isoelectronic series and small molecules are reported and compared with *ab initio* wave-function calculations. Particular attention is paid to the quality of approximations to the exchange-only optimized effective potential (OEP) approach: we consider both the Localized Hartree Fock as well as the Krieger-Li-Iafrate methods. Analysis of density differences at the exchange-only level reveals the impact the approximations have on the resulting electronic densities. These differences are further quantified in terms of the ground state energies, frontier orbital energy differences and highest occupied orbital energies obtained. At the correlated level an OEP approach based on a perturbative second-order correlation energy expression is shown to deliver results comparable with those from traditional wave function approaches, making it suitable for use as a benchmark against which to compare standard density-functional approximations.

I. INTRODUCTION

The accuracy of density functional theory (DFT) within the Kohn-Sham (KS) approach (KS-DFT)¹ is strongly dependent on the approximations used in practical exchange-correlation (XC) functionals. Although formally an exact theory, based on the Hohenberg-Kohn theorems², after four decades of growing applications and success, it still struggles with the problem of defining theoretically correct, non-empirical, robust and practically applicable XC functionals. In the last decade, significant attention has been given to the use of orbital-dependent XC functionals in the KS methodology at both the exchange³⁻¹⁴ and correlation¹⁵⁻³³ levels, which open up new routes in the search for new DFT methods.

The use of orbital-dependent functionals naturally leads to the optimized effective potential (OEP) method^{34,35}, which defines local KS potentials^{3,15,16,36} (for a review see³⁷⁻³⁹). To develop orbital-dependent functionals experience from wave function theories (WFTs) can be exploited to define a series of XC approximations that systematically converge towards the full configuration interaction (FCI) limit⁴⁰⁻⁴². This concept has been named *ab initio* DFT¹⁷ and has proven to be a very effective route for defining and deriving orbital-dependent exchange-correlation functionals and potentials. Recent applications of *ab initio* DFT^{16,17,24} show that these functionals are free of many of the limitations of standard DFT. There is no self interaction error problem, they provide qualitatively correct exchange-correlation potentials, total and correlation energies and ionization potentials. They have also been successfully applied to the description of van der Waals interactions⁴³ and systems with quasidegeneracy^{24,27}.

Recently the concept of difference radial-density (DRD) distributions, defined with respect to the

Hartree-Fock (HF) radial density⁴⁴, has been used to compare the electronic densities calculated from DFT approaches (both standard and orbital-dependent) and WFT methods. In fact, it has been shown that the DRD distribution

$$\text{DRD}(r) = 4\pi r^2 [\rho(r) - \rho^{\text{HF}}(r)] , \quad (1)$$

with ρ any DFT or WFT density and ρ^{HF} the Hartree-Fock density, can provide a useful tool in the development and testing of new and existing exchange-correlation functionals in KS-DFT. Based mainly on the DRD analysis it was shown^{42,44,45} that VWN⁵⁴⁶, LYP⁴⁷ and other correlation functionals do not individually represent substantial dynamic correlation effects in the KS potential or electron density. Additionally, we have demonstrated that at the exchange-only level of approximation, popular standard DFT exchange functionals, in addition to their nominal role, represent some dynamic correlation effects^{44,45}.

In this paper we consider this analysis further and apply it to a range of orbital-dependent exchange-only and exchange-correlation approximations. At the exchange-only level we consider electronic densities calculated using the Localized HF (LHF)⁹ and Krieger-Li-Iafrate (KLI)³ approximations. The DRDs constructed for these approaches are compared with those from exchange-only OEP as well as correlated *ab initio* DFT and WFT methods. The impact of the approximations involved in the LHF and KLI approaches on the DRDs are analysed in light of these comparisons. Additionally, the quality of each approach is assessed in terms of its associated total energy and the accuracy of the differences of highest occupied molecular orbital (HOMO) energy and lowest unoccupied molecular orbital energy (LUMO), the HOMO-LUMO gap. The latter provides a sensitive probe of the

quality of the underlying KS effective potential. Accurate data for the HOMO–LUMO gaps are obtained by employing an inversion approach⁴⁸ using coupled–cluster singles–doubles and perturbative triples [CCSD(T)] densities.

II. METHODOLOGY

In order to define orbital–dependent XC functionals, potentials and correlated OEP–KS equations we will follow the idea of *ab initio* DFT¹⁷, in which the density condition³⁶ together with coupled–cluster (CC) methodology is employed to derive orbital–dependent multiplicative exchange–correlation potentials in the KS–OEP approach, defining a range of exchange–only and correlated OEP methods.

The KS density condition^{36,49} states that, since by construction the KS determinant Φ_{KS} provides the exact density at a given space–spin coordinate, any corrections to the converged KS density, introduced by changes in $\varphi_i(\mathbf{r})$, must vanish^{17,36},

$$\rho(\mathbf{r}) = \rho^{\text{KS}}(\mathbf{r}) + \delta\rho^{\text{KS}}(\mathbf{r}), \quad \delta\rho^{\text{KS}}(\mathbf{r}) = 0. \quad (2)$$

The density corrections $\delta\rho^{\text{KS}}(\mathbf{r})$ are written using the density matrix correction $\Delta\gamma_{pq}$ from CC theory⁵⁰ or many–body perturbation theory (MBPT), and then can be expanded by orders in the perturbation V by separating the total Hamiltonian,

$$H = \sum_i h(i) + \sum_{i<j} 1/r_{ij} \quad (3)$$

into a zeroth–order part H_0 and a perturbation V ,

$$H = H_0 + V, \quad V = H - H_0 \quad (4)$$

For the detailed diagrammatic and algebraic derivation of working correlated OEP equations see Refs. 17,18,22,24.

The density condition at first order, $\delta\rho^{(1)}(\mathbf{r}) = 0$, leads to the exchange–only OEP (OEPx) equation,

$$\sum_{ai} \varphi_a(\mathbf{r}) \varphi_i^*(\mathbf{r}) \left[\frac{\langle a|\hat{K} + v_x|i\rangle}{\varepsilon_i - \varepsilon_a} \right] = 0, \quad (5)$$

where \hat{K} is the nonlocal HF exchange potential. Throughout this work i, j, \dots denote occupied orbitals, a, b, \dots unoccupied orbitals and p, q, \dots are used for general (i.e. occupied or unoccupied) orbitals. The multiplicative exchange–only OEP potential, $v_x(\mathbf{r})$, corresponds to the functional derivative of the exchange–only energy functional, $E_x[\varphi_{\text{KS}}]$, which has the form of the usual exchange–energy functional from HF theory evaluated on KS orbitals:

$$E_x[\varphi_{\text{KS}}] = -\frac{1}{2} \sum_{i,j} (ij|ji), \quad (6)$$

with the two electron integrals defined as

$$(pq|rs) = \int \varphi_p^*(\mathbf{r}) \varphi_q(\mathbf{r}) \frac{1}{|\mathbf{r} - \mathbf{r}'|} \varphi_r^*(\mathbf{r}') \varphi_s(\mathbf{r}') d\mathbf{r} d\mathbf{r}'. \quad (7)$$

The KS orbitals employed are the solutions to the standard KS equation

$$\left[-\frac{1}{2} \nabla^2 + v(\mathbf{r}) + \int \frac{\rho(\mathbf{r}')}{|\mathbf{r} - \mathbf{r}'|} d\mathbf{r}' + v_{\text{xc}}[\rho](\mathbf{r}) \right] \varphi_p(\mathbf{r}) = \varepsilon_p \varphi_p(\mathbf{r}), \quad (8)$$

where $v(\mathbf{r})$ is the external potential due to the nuclei, the third term is the classical Coulomb potential and $v_{\text{xc}}(\mathbf{r})$ is the local exchange–correlation potential.

Fulfilling the requirement of Eq. (2) through second–order, $\delta\rho^{(2)}(\mathbf{r}) = 0$, allows the definition of the orbital–dependent OEP2 equations for the second–order correlation potential. In this paper we will use the OEP2–sc¹⁷ variant of this approach. The OEP2–sc correlation functional takes the standard form of the second–order energy expression in many–body perturbation theory [MBPT(2)],

$$E_c^{(2)} = \frac{1}{2} \sum_{i,j,a,b} \frac{|(ia|jb)|^2}{d_{ijab}} - \frac{1}{2} \sum_{i,j,a,b} \frac{(ia|jb)(aj|bi)}{d_{ijab}} + \sum_{i,a} \frac{|f_{ia}|^2}{d_{ia}}. \quad (9)$$

where the denominators are defined as

$$d_{ia} = f_{ii} - f_{aa} \quad \text{and} \quad d_{ijab} = f_{ii} + f_{jj} - f_{aa} - f_{bb}, \quad (10)$$

where f_{pq} are the usual Fock matrix elements defined in terms of KS–OEP spin–orbitals,

$$f_{pq} = \varepsilon_p^{\text{KS}} \delta_{pq} - \langle p|\hat{K} + v_{\text{xc}}|q\rangle. \quad (11)$$

For OEP2–sc the semi–canonical (SC) transformation of the OEP2–KS orbitals is performed⁵⁰, to reinstate orbital invariance of the MBPT(2) energy for rotations which mix occupied or virtual orbitals among themselves.

This method has been found to provide a stable alternative to the other second–order correlated OEP2–KS theories^{17,27,41–43}, where problems with convergence, overestimation of the correlation energy, and in many cases poor quality of the correlation potentials were encountered^{19,21,24,27,42}. Recently the scaled–opposite–spin version of the second–order correlated OEP method (SOS–OEP2) was also proposed³³.

In order to solve the OEP equations to determine the exchange–correlation potential, which is then used in the iterative self–consistent–field (SCF) solution of the KS equations (see Eq. (8)), we use the finite basis set implementation of the OEP method from Refs. 6,7. It involves a projection method^{7,51} for solving the required integral equation, and by construction all potentials are expanded in terms of auxiliary Gaussian functions.

To minimize computational difficulties that are often encountered in the application of the finite basis set OEP procedure to both the exchange–only energy

functional^{8,12,14,52–56} and that including correlation^{18,24}, which are the manifestation of the well-known instability associated with numerical solutions of Fredholm integral equations of the first kind, we use the same carefully chosen uncontracted basis sets to represent both the orbitals and potentials in our procedure^{8,17,24,27,51}. These issues have been discussed extensively in the literature and several schemes have been proposed for managing this problem^{12,14,52–57}. Since we use finite Gaussian-type basis sets, which at large r decay much faster than $1/r$, an incorrect asymptotic behaviour of our exchange–correlation potentials (which should decay as $-1/r$) would be obtained. To ensure the correct asymptotic behaviour we use the Colle–Nesbet⁵⁸ decomposition of the exchange–correlation OEP potential into two components,

$$v_{xc}(\mathbf{r}) = v_{\text{Slater}}(\mathbf{r}) + \sum_t^{N_{\text{aux}}} c_t g_t(\mathbf{r}), \quad (12)$$

The first term

$$v_{\text{Slater}}(\mathbf{r}) = - \sum_{ij} \frac{\phi_i^*(\mathbf{r})\phi_j(\mathbf{r})}{\rho(\mathbf{r})} \int d\mathbf{r}' \frac{\phi_j^*(\mathbf{r}')\phi_i(\mathbf{r}')}{|\mathbf{r}-\mathbf{r}'|} + \text{c.c.} \quad (13)$$

is the Slater potential⁵⁹, which is responsible here for preserving the $-1/r$ asymptotic behaviour and is calculated on a grid. The second component is determined via the OEP integral equation, where $g_t(\mathbf{r})$ are the auxiliary Gaussian basis functions and c_t are the expansion coefficients.

An alternative approach that approximates the exchange-only OEP potential is the so called localized Hartree–Fock (LHF) method^{9,60}. In this method a local exchange potential is derived starting from the approximate assumption that the HF and the exact-exchange Slater determinants are equal⁹. The resulting LHF exchange potential is

$$v_x^{\text{LHF}}(\mathbf{r}) = v_{\text{Slater}}(\mathbf{r}) + \sum_{i,j} \phi_i(\mathbf{r})\phi_j(\mathbf{r}) \times \int \phi_i(\mathbf{r}') \left[\sum_k \frac{\phi_k(\mathbf{r})\phi_k(\mathbf{r}')}{|\mathbf{r}-\mathbf{r}'|} - v_x^{\text{LHF}}(\mathbf{r}') \right] \phi_j(\mathbf{r}') d\mathbf{r}', \quad (14)$$

where the molecular orbitals are assumed to be real. The second term on the right hand side is the so called correction term and in its calculation the HOMO element must be excluded from the double summation (as indicated by the prime) to enforce the correct asymptotic behaviour of the LHF potential⁹. If all the $i \neq j$ terms are dropped from the summations in Eq. (14), the KLI potential³ is recovered. We note that, despite the fact that the LHF potential is not a functional derivative of any energy functional^{61,62}, it is computationally very stable and generally regarded as a very good approximation to the KS exact exchange potential, having been applied to a range of different problems in quantum chemistry^{63–70}.

Moreover, it is also derived within the common energy denominator approximation (CEDA)¹⁰ and effective local potential (ELP)¹² methods as well as the first order approximation to a linear Sham–Schlüter equation²⁵. However, some studies have noted that the subtle differences between the OEP exchange only and LHF/KLI potentials can have significant effects in the calculation of response properties^{71–73}. The quality of the LHF/KLI approximations is further examined in the present work.

To analyze the performance of the orbital-dependent and standard KS–DFT methods, we use as a reference the electronic densities calculated at the exchange-only (HF) level, at the second-order Møller–Plesset (MP2) and coupled-cluster singles–doubles with perturbative triples (CCSD(T)) levels.

A. Computational Details

To compare the quality of different WFT and DFT methods, we have performed calculations for several representative systems, which can be divided into three classes: i) atoms (He, Be, Ne, Ar), ii) the neon isoelectronic series (Si⁴⁺, Ca¹⁰⁺, Zn²⁰⁺), without relativistic corrections, and iii) small molecules (He₂, N₂, CO, H₂O).

The calculations have been performed using different computational approaches. In the *ab initio* DFT category we used the exchange-only OEPx and correlated OEP2–sc methods, as implemented in the ACES II package⁷⁴. The OEP equations were solved in a fully self-consistent manner together with the KS equations until a final convergence criteria of 10^{-8} a.u. on the maximum change in density matrix elements is reached.

As effective exact-exchange methods we considered the orbital-dependent LHF and KLI, as implemented in the TURBOMOLE program package⁷⁵. The Slater potential was computed numerically⁶⁰ and the correction term using the conjugate gradient technique⁹. Hartree-Fock orbitals have been used as starting orbitals for LHF/KLI calculations, giving convergence in less than 10 SCF cycles for all systems considered in this work. The energy and density convergence criteria were set to 10^{-6} a.u.

Among the standard *ab initio* WFT methods, MP2 and CCSD(T) calculations have been employed to calculate correlation energies and electronic densities.

The inverse-KS calculations were performed with a development version of the DALTON2011 quantum chemistry program⁷⁶. The electronic densities for the MP2 and CCSD(T) methods are obtained from relaxed density matrices^{77–80} constructed using the Lagrangian approach^{81–84}. In order to determine reference KS potentials, eigenvalues and HOMO–LUMO gaps corresponding to the WFT densities we have employed the inversion approach of Yang and Wu⁴⁸. We employ the same uncontracted basis sets for the expansion of the potential and orbitals in this approach. The Fermi–Amaldi potential is used to ensure correct asymptotic decay of the calculated XC potentials. The smoothing norm pro-

cedure of Heaton–Burgess *et al.*^{13,57} was employed with a regularisation parameter of 10^{-5} and the calculations were considered converged when the gradient norm was below 10^{-8} a.u. For further details see Refs. 42,48. The HOMO energies and HOMO–LUMO gaps determined from these calculations for the MP2 and CCSD(T) densities are labelled KS[MP2] and KS[CCSD(T)], respectively.

1. Basis-sets

The selection of the basis sets in this work was mainly dictated by the requirement of smooth and well-behaved convergence of the OEP calculations. For this reason all basis sets were constructed by partial or full uncontraction of medium size (triple zeta) basis sets originally developed for correlated calculations. The choice of the basis functions and the de-contraction schemes were optimized to ensure a smooth behaviour of OEP potentials, especially because in all calculations where the KS potentials needs to be expanded in terms of Gaussian basis functions the same basis sets was employed for the potential expansion as for the molecular orbitals.

In more detail, an even tempered 20s10p2d basis was employed for He atom and He₂ molecule; the uncontracted ROOS–ATZP⁸⁵ basis was used for Ne; for the Be atom the ROOS–ATZP basis set was used with s and p functions uncontracted; for Ar the uncontracted ROOS–ATZP⁸⁵ basis is used for s and p type basis functions, whereas for *d* and *f* orbitals we used the uncontracted aug-cc-pwCVQZ⁸⁶ basis set. The uncontracted cc-pVTZ basis set of Dunning⁸⁷ was used for the molecular systems N₂, CO and H₂O. For the neon isoelectronic series members the following basis sets were used: in case of Si⁴⁺ the ROOS–ATZP basis set with s and p functions uncontracted; for Ca¹⁰⁺ ion we used uncontracted ROOS–ATZP basis set of Ne; the Zn²⁰⁺ ion was calculated in the ROOS–ATZP basis set with s functions uncontracted and the g functions removed.

We remark that with this choice of the basis sets, especially for ionic systems, our HF and CCSD(T) results differ from benchmark results^{88,89}. Nevertheless, because the main goal of the present work is to perform a relative (and mostly qualitative) comparison between different methods and because all the exchange-only as well as all the XC methods considered here have a similar basis set convergence behaviour (almost linear for exchange and cubic for correlation), the analysis of the different results is expected to be only slightly influenced by this issue. Thus, the present computational set up should allow fair comparison and assessment of the different approaches.

III. RESULTS

In this section we compare a range of orbital-dependent exchange-only and exchange-correlation functionals with reference results from WFT methods. Different criteria are used to assess the quality of the approaches. Firstly in Section III A, we assess the accuracy of the total energies delivered by each method. Then we consider in Section III B the density differences (DRDs for atomic systems) relative to Hartree-Fock to assess both the impact of correlation and the effect of approximations in the derivation of KS-potentials on the electronic density obtained. Finally, in Section III C we compare the HOMO-LUMO gaps and HOMO energies calculated for each approach.

A. Total energies

The total ground state energies are presented in Table I. For each method the mean absolute error (MAE) with respect to the reference values (Hartree-Fock and CCSD(T) results for exchange-only and exchange-correlation methods, respectively) are also reported. The MAEs are separated for each class of systems (atoms, neon isoelectronic series, molecules). The total MAE is also reported in the last line of Table I.

Considering exchange-only methods, we see that they all perform very similarly and are extremely close to the reference HF results. This finding indicates the high quality of these approaches for the description of energetic properties of electronic systems. In closer detail, we observe that the OEPx method delivers the smallest deviations from HF, as expected. Instead, because of the variational principle, LHF and KLI results are systematically slightly above the HF energy (except for case of He, which gives exactly the same energy, by definition). Nevertheless, the LHF and KLI approximations show reasonable agreement with the OEPx results for the neutral atomic and molecular systems, typical differences between HF and LHF/KLI being below 8 mH. Overall, the results of Table I show that LHF and KLI have a fairly similar performance, with error measures approximately twice as large as OEPx. Moreover, the deviations obtained with LHF are slightly smaller than the ones yielded by KLI. In this respect, it should be noted that both methods employ the same (i.e. Hartree-Fock) total energy expression but different (non-variational) potentials. Thus, the difference between LHF and KLI originates only from self-consistent effects. In addition, it is worth noting that the KLI potential is not invariant with respect to orbital rotations, whereas the LHF energy is stable in this respect⁹.

Considering the full exchange-correlation approaches we can see that the OEP2-sc method reproduces MP2 results quite well and both have small deviations with respect to CCSD(T), with a total MAE of about 10-12 mH. This behaviour can be attributed to the fact that

TABLE I: Total energies (in Hartree) for Hartree-Fock and CCSD(T) methods. Differences (in mHartree) from these reference values are shown for several exchange-only (X-only) and exchange-correlation methods, respectively. Mean absolute errors (MAE) are reported for all systems as well as for the atomic, neon isoelectronic series and the molecular systems.

System	X-only methods				XC methods		
	HF	OEPx	LHF	KLI	CCSD(T)	MP2	OEP2-sc
He	-2.8617	0.0	0.0	0.0	-2.9025	5.6	5.6
Be	-14.5730	0.6	0.6	0.7	-14.6619	19.9	19.7
Ne	-128.5466	1.6	2.3	2.2	-128.9000	7.5	5.9
Si ⁴⁺	-285.1801	1.2	7.7	7.7	-285.3462	2.4	2.1
Ca ¹⁰⁺	-640.3120	1.9	3.1	3.3	-640.5276	3.1	3.0
Zn ²⁰⁺	-1552.5576	0.8	2.5	2.9	-1552.7104	1.4	1.4
Ar	-526.8165	5.3	7.1	7.2	-527.4575	23.9	22.0
He ₂	-5.7234	0.0	0.0	0.0	-5.8051	11.1	11.1
N ₂	-108.9847	5.3	7.5	7.7	-109.4763	20.1	11.6
CO	-112.7816	5.2	7.2	7.4	-113.2574	23.5	14.5
H ₂ O	-76.0578	2.0	3.2	3.5	-76.3869	14.9	12.7
MAE _{ato}		1.9	2.3	2.5		14.2	13.3
MAE _{iso}		1.4	3.6	4.0		3.6	3.1
MAE _{mol}		3.1	4.5	4.6		17.4	12.5
MAE _{tot}		2.2	3.7	3.9		12.1	10.0

OEP2-sc has a second-order correlation potential based on the MBPT(2) type energy functional. Interestingly, the OEP2-sc MAEs are also slightly lower than the MP2 ones, which may be a result of the correlation effects included in the orbitals by relaxation during the self-consistent solution of the KS-OEP equations. Examining the differences between the errors for different classes of systems, it is interesting to note that the neon isoelectronic series gives MAEs 4-5 times smaller than the ones for the atomic and molecular systems, for both the MP2 and OEP2-sc methods. This result can be understood from the relatively simple behaviour of the correlation energies for the heavier ions^{88,89}, which are very well described by second-order perturbation theory.

B. Density-based Analysis

For a more detailed comparison about the potential of orbital-dependent methods, we directly compare the DRD distributions calculated relative to the HF radial densities for the atomic systems. This allows us to inspect the influence of correlation effects on the density.

In Figure 1 we compare DRDs for the neon atom, calculated using orbital-dependent KS functionals (OEPx, KLI, LHF and OEP2-sc; top panel) and wave function theory methods (MP2 and CCSD(T); middle panel). We also report, for comparison, (semi-)local standard DFT methods (SVWN5^{46,90}, BLYP^{47,91}; bottom panel). The CCSD(T) plots are our reference results.

Examining the plots we note that the OEPx DRD is flat and almost overlaps with the x -axis (the OEPx den-

sity is almost identical to HF one). Including correlation in the orbital-dependent calculations at the OEP2-sc level provides a DRD that closely resembles the reference MP2 and CCSD(T) results. The SVWN5 and BLYP results in Figure 1 show a similar behaviour to the reference CCSD(T) DRD, except for their amplitudes, which are much larger than the CCSD(T) results. However, this reasonable overall behaviour arises because dynamic correlation effects are represented mainly by the exchange-only S and B88 functionals, which dominate DRDs obtained from the total exchange-correlation SVWN5 and BLYP calculations respectively^{44,45}.

Interestingly, the LHF and KLI DRDs in Figure 1 are not as flat as may be expected based on the analysis of their total energies as presented in Section III A. It appears that for $r < 1$. a.u. the LHF/KLI approximations lead to substantial differences in the DRDs relative to HF but that their accuracy improves rapidly as r increases. Furthermore, these errors give rise to a DRD profile that to some extent mimics correlation effects at small r . Examining the top panel in Figure 1 we see that first downward peak (at $r \approx 0.08$ a.u.) is also present in the SVWN5 result. This peak corresponds to a large density deviation at the nucleus (i.e. LHF/KLI has less density at the nucleus than HF): however due to the radial factor in Eq. (1) it appears as a small peak at finite r (see also section III B 2). The following upward peak (at $r \approx 0.28$ a.u.) in the inter-shell region closely resembles the one of OEP-sc, MP2 and reference CCSD(T). The outer features of the correlated DRDs are however not mimicked at the KLI/LHF level. Similar observations were made by Teale and Tozer in Ref. 73

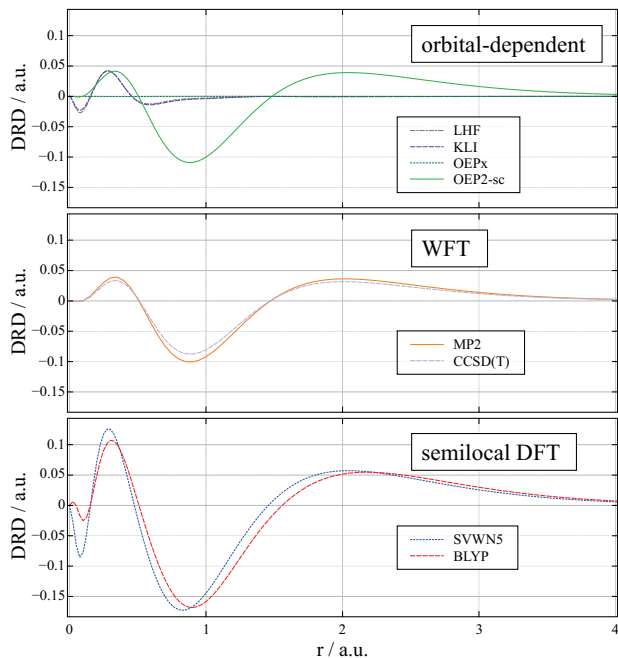


FIG. 1: Difference radial density distributions (DRD; see Eq. (1)) for the neon atom, calculated using orbital-dependent OEP-DFT functionals (top panel) wave function theory (WFT) methods (middle panel) and semi-local standard DFT methods (bottom panel).

and used to interpret the fact that LHF and KLI approaches yielded unexpectedly accurate NMR shielding constants in Refs. 71 and 72. Whilst energetically the LHF and KLI approximations are reasonably accurate their potentials are not the functional derivative of the orbital-dependent exchange energy with respect to the density. Instead errors (relative to OEPx) associated with the approximations used in their derivation lead to potentials that give rise to densities with errors at small r in the core and near valence regions, as manifested in the DRDs. The results here may go some way to further explaining the results in Refs. 71 and 72 for NMR parameters, since these properties are sensitive only to regions close to nuclei and in these areas the LHF and KLI results mimic correlation effects. This may explain why the calculated values exhibit a quality closer to correlated GGA results than to OEPx.

1. Neon isoelectronic series

To analyse the behaviour of the different approximations in more detail, we present similar plots for a few members of the neon isoelectronic series i.e. Si^{4+} , Ca^{10+} , Zn^{20+} and Ne atom in Figure 2. For clarity we present results obtained from different methods in separate panels. Moreover, we do not report KLI and OEPx results here, because they are essentially indistinguishable from

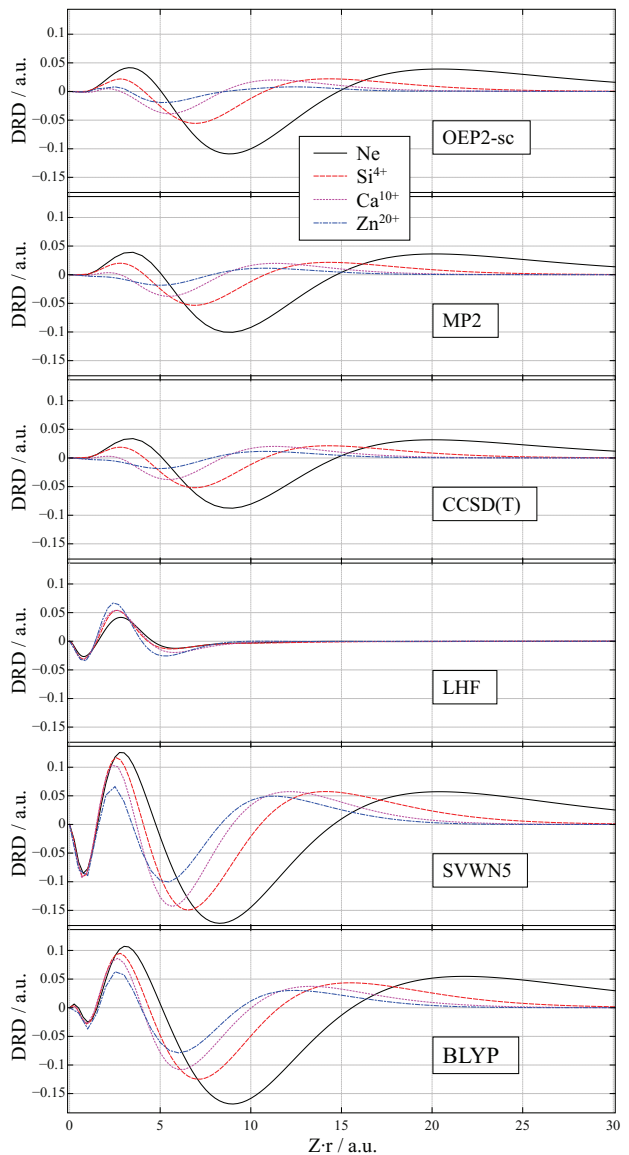


FIG. 2: Difference radial density distributions (DRD; see Eq. (1)) for the Ne atom and a few members of the neon isoelectronic series (Si^{4+} , Ca^{10+} and Zn^{20+}), calculated using orbital-dependent OEP-DFT functionals (OEP2-sc, KLI and LHF), wave function theory methods (MP2 and CCSD(T)) and semi-local standard DFT methods (SVWN5, BLYP). Note that on the x -axes the radial coordinate r has been scaled by the nuclear charge, Z .

LHF and HF results, respectively, on the scale presented. We observe that a clear trend can be distinguished for CCSD(T) and MP2. The DRDs become, of course, more compact with increasing Z values (note that in the plot Zr is reported on the x -axis). At the same time the height of the different peaks is reduced with Z . This trend is more accentuated for core features that are almost invisible (on this scale) already for Ca^{10+} . The reference trend is well reproduced by the OEP2-sc calculations. Thus, this method proves to describe the change

in correlation effects on increasing Z with good accuracy and reliability.

The same trend is also qualitatively reproduced by pure DFT functionals. However, these approaches fail to give a correct quantitative description of the DRDs of the different members of the isoelectronic series: i) the amplitude of the oscillations is overestimated, ii) the decrease of the peak height with Z is slower and iii) an additional downward peak is observed near the origin.

In contrast, the LHF calculations display a completely different behaviour. In this case, in fact, the DRD peak position is almost fixed at $Zr \approx 2.5 - 2.8$ a.u. and the amplitude of the DRD oscillations is almost constant (actually slightly increasing with increasing values of Z). This is opposite to what can be expected on the basis of the accurate CCSD(T) calculations and so the effect of LHF mimicking correlation breaks down as Z increases. These results show therefore that the LHF potential does not in general include proper correlation effects, as expected from an orbital-dependent exchange-only method. Rather, the features of the DRD plots can be traced back to some limitations of the correction term which cannot mimic accurately the exact-exchange response term in the 1s-2s inter-shell region. On the other hand, the fact that the DRD profiles are almost independent from Z and vanish in the valence region means that the LHF potential deviation from the OEPx potential is only due to an almost constant term near the core region. This error is therefore quite systematic and LHF can be safely used as a reasonable approximation to investigate exact-exchange in heavy ions.

2. Molecules

The density-based analysis presented so far for atoms using DRDs, can be carried out also for molecules by considering density differences just along one line. To show this we report in Figure 3 the density difference along the molecular axis of a CO molecule, relative to HF, for different theoretical approaches. The shape of the accurate MP2 and CCSD(T) density differences reflects a depletion of the density around the carbon atom and an increase around the oxygen atom relative to HF. This in turn reflects the fact that HF theory predicts a qualitatively incorrect dipole moment for CO (-0.104 a.u. for HF compared with $+0.111$ a.u. for MP2), which is corrected in the correlated methods by a redistribution of charge. We see once again that the OEP2-sc method can reproduce the reference CCSD(T) and MP2 results with good accuracy. In contrast, both LHF and the conventional DFT functionals show large density-difference peaks around nuclei which are however also present in atomic systems, see Section III B. The LHF density-difference profile has qualitatively more in common with SVWN5 whereas in BLYP the peaks near the nuclei are of opposite sign. This is consistent with the

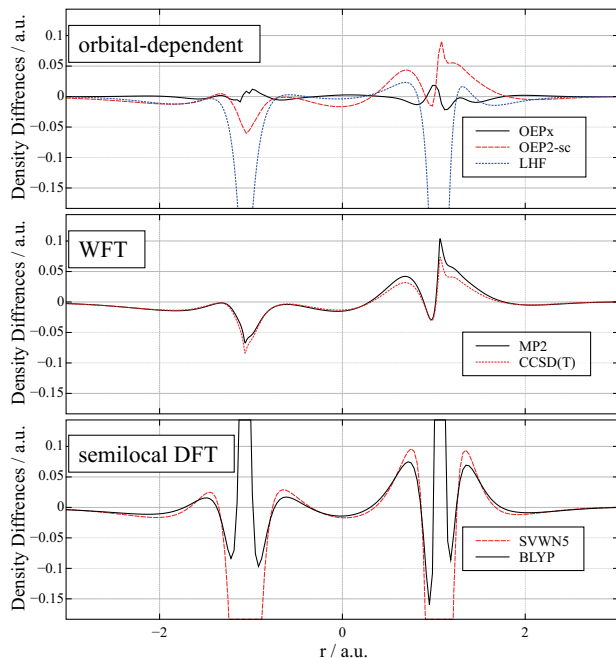


FIG. 3: Difference total density distributions (along the molecular axis) relative to HF, for the CO molecule, calculated using orbital-dependent OEP-DFT functionals (top panel) wave function theory methods (middle panel) and semi-local standard DFT methods (bottom panel).

analysis in Ref. 73.

C. KS HOMO-LUMO gaps and Ionization Potentials

To complete our analysis we consider the KS HOMO-LUMO gaps and HOMO energies delivered by each of the methods in comparison with accurate values obtained from KS[CCSD(T)] calculations. The latter have been used here as reference values for the orbital energies and energy-gaps to allow a direct comparison between all of the methods using the same finite Gaussian basis sets. For many of the systems considered here benchmark estimates of the orbital energies may be found in Refs. 92–97. However, these values are calculated using a range of different basis sets and different methodologies to obtain accurate densities, making consistent comparisons with our data difficult. Nonetheless we note that our values are broadly consistent with those in Refs. 92–97.

The KS HOMO-LUMO gaps for each approach are presented in Table II. The exchange-only methods show in general an overestimation with respect to the KS[CCSD(T)] values. However, for argon and beryllium the opposite trend is obtained. This shows that the correlation effects are subtle in this context and cannot be easily predicted. For the atomic and ionic systems the LHF and KLI gaps are rather close to the OEPx ones. For molecules the gaps are reduced compared to OEPx

TABLE II: HOMO–LUMO gaps (in eV) from various methods (see text for further details). Mean absolute relative errors (MARE) with respect to KS[CCSD(T)] values are presented for the full set of systems as well as for the subsets corresponding to neutral atoms (ato), the members of the neon isoelectronic series (iso) and molecular systems (mol).

System	OEPx	OEP2-sc	KLI	LHF	KS[MP2]	KS[CCSD(T)]
He	21.60	21.32	21.67	21.67	21.33	21.21
Be	3.57	3.64	3.54	3.54	3.63	3.61
Ne	18.48	16.45	18.47	18.48	16.81	17.00
Si ⁴⁺	104.02	100.61	105.11	105.11	102.37	102.45
Ca ¹⁰⁺	348.35	346.03	349.43	349.43	346.13	346.17
Zn ²⁰⁺	1056.56	1046.56	1055.78	1055.76	1052.45	1052.43
Ar	11.41	11.43	11.06	11.09	11.45	11.51
He ₂	21.28	21.02	20.82	20.82	20.43	20.31
N ₂	9.21	8.37	8.73	8.78	8.41	8.51
CO	7.77	7.22	7.32	7.31	7.27	7.25
H ₂ O	8.47	7.51	8.52	8.32	7.55	7.71
MARE _{ato}	3.1%	1.3%	4.2%	4.1%	0.7%	
MARE _{iso}	0.9%	0.8%	1.3%	1.3%	0.0%	
MARE _{mol}	7.5%	2.0%	4.1%	3.6%	1.0%	
MARE _{tot}	4.1%	1.4%	3.4%	3.2%	0.6%	

and so move closer to the KS[CCSD(T)] values, leading to an overall reduction in the error measures: the mean absolute relative error for molecules (MARE_{mol}) is reduced from 7.5% in OEPx to 3.6% in LHF.

The OEP2-sc method leads to a substantial improvement of the HOMO-LUMO gaps, thanks to the inclusion of correlation. In particular it yields smaller gaps than OEPx for all the systems except beryllium and argon, in line with the reference values. Thus, it appears to be able to provide a qualitatively correct description of correlation effects in all systems, unlike conventional DFT correlation functionals which always increase the HOMO-LUMO gap²⁵. However, this result may benefit from a strong cancellation of systematic errors as indicated by the analysis of HOMO energies (see below). Moreover, the OEP2-sc correlated approach leads for many systems to a too strong reduction of the gap, resulting in an underestimation of the KS[CCSD(T)] values. This makes it somewhat further from the KS[CCSD(T)] values than KS[MP2]. This finding supports the idea that OEP2-sc results for the HOMO–LUMO gap should be treated with caution and may also indicate that the orbital relaxation effects incorporated in OEP2-sc have a significant effect on determining the Kohn–Sham eigenvalue spectrum. Nevertheless, overall OEP2-sc is the best of the DFT approaches considered in the present work and is substantially more accurate than typical conventional DFT functionals.

In Table III we present the HOMO energies together with their MAREs, obtained with the same methods as in Table II. In this case, all the exchange–only methods (HF, LHF, KLI, OEPx) perform rather well compared with KS[CCSD(T)] and with similar accuracy

(MARE_{tot} below 9%). The KLI and LHF HOMO energies are very close to each other and slightly closer to the KS[CCSD(T)] values, whereas OEPx is slightly more similar to HF, consistent with the results in the previous sections. On the other hand, the correlated OEP method (OEP2-sc), despite being the best DFT approach, provides only slightly more accurate results relative to KS[CCSD(T)] than OEPx. In fact, its MARE_{tot} is 8% and thus much larger than for KS[MP2] (MARE_{tot}=1.5%). Considering the molecular results, the MARE_{mol} value is much larger for OEP2-sc than for KS[MP2] and the individual values are substantially different to the KS[CCSD(T)] reference values. Orbital energies are particularly sensitive to the quality of the underlying exchange–correlation potentials and these results indicate that the OEP2-sc potential may be improved in this respect. This is particularly clear when comparing the OEP2-sc and KS[MP2] HOMO eigenvalues. The densities for these two approaches are typically very similar (see Figures 1- 3), whilst their HOMO eigenvalues differ substantially. For N₂ and H₂O the effect of OEP2-sc correlation is to make the HOMO eigenvalue more negative than OEPx, whilst the reference values are more positive. Given the sensitivity of the HOMO eigenvalue to the exchange–correlation potential this type of comparison may be a useful further test of other *ab initio* DFT functionals.

IV. CONCLUSIONS

In this work we have presented a density-difference based analysis of orbital–dependent exchange and

TABLE III: HOMO energies (in eV) obtained from various methods (see text for further details). Mean absolute relative errors with respect to the KS[CCSD(T)] values are also presented for the full set of systems as well as for the subsets corresponding to neutral atoms (ato), the members of the neon isoelectronic series (iso) and molecular systems (mol).

	OEPx	OEP2-sc	KLI	LHF	HF	KS[MP2]	KS[CCSD(T)]
He	-24.98	-24.70	-24.99	-24.99	-24.99	-24.68	-24.56
Be	-8.41	-8.66	-8.34	-8.41	-8.42	-9.07	-9.43
Ne	-23.15	-20.97	-23.11	-23.12	-23.14	-21.01	-21.14
Si ⁴⁺	-168.53	-161.40	-168.46	-168.47	-168.52	-164.08	-164.16
Ca ¹⁰⁺	-593.40	-590.37	-593.33	-593.33	-593.38	-586.49	-586.51
Zn ²⁰⁺	-1847.95	-1823.08	-1843.90	-1843.88	-1847.93	-1826.46	-1826.30
Ar	-16.07	-15.66	-16.03	-16.06	-16.08	-15.47	-15.58
He ₂	-24.98	-24.70	-24.83	-24.83	-24.98	-22.74	-22.62
N ₂	-17.16	-18.30	-17.12	-17.08	-16.67	-14.93	-13.96
CO	-15.02	-14.65	-15.01	-14.97	-15.07	-13.56	-13.17
H ₂ O	-13.70	-14.25	-13.58	-13.66	-13.75	-11.44	-11.53
MARE _{ato}	6.3%	2.5%	6.4%	6.2%	6.3%	1.4%	
MARE _{iso}	1.7%	0.8%	1.6%	1.6%	1.7%	0.0%	
MARE _{mol}	16.6%	18.8%	16.0%	16.1%	15.9%	2.8%	
MARE _{tot}	8.8%	8.0%	8.6%	8.5%	8.5%	1.5%	

exchange–correlation functionals in KS-DFT. The use of *ab initio* DFT methods via the OEP approach gives a partitioning of exchange and correlation contributions much more in line with standard *ab initio* WFT methods. Comparison of OEPx and HF densities showed that exact-exchange-only DFT densities are very similar to those obtained from HF. This is also reflected in the comparison of their energies and HOMO eigenvalues. We also considered the LHF and KLI approximations to OEPx. These approaches deliver exchange and total energies that are close to that of OEPx and HF, however, examination of DRDs relative to HF revealed substantial differences between the LHF/KLI and HF densities. In particular, their densities differ in the core and inner-valence regions close to nuclei. Although they remain accurate in the outer valence and asymptotic regions.

To assess the accuracy of exchange–correlation functionals the DRDs associated with MP2 and CCSD(T) theories were constructed and compared with standard DFT results and the correlated OEP2-sc approach for the neon atom and three members of the neon isoelectronic series. The standard DFT distributions showed a reasonable qualitative reproduction of the CCSD(T) DRDs though their amplitudes were not highly accurate. The OEP2-sc method delivers results of good accuracy very close to the MP2 DRDs, as may be expected. Interestingly, for neon the LHF and KLI DRDs show features close to the nucleus that appear to mimic correlation effects in that region. To examine this further the Si⁴⁺, Ca¹⁰⁺ and Zn²⁰⁺ members of the neon isoelectronic series were investigated. Here similar conclusions were obtained for the standard DFT functionals which qualitatively reproduce the MP2 and CCSD(T) DRDs and also

for the OEP2-sc method which closely reproduces the WFT DRDs as Z increases. However, for LHF and KLI as Z increases the qualitative behaviour of the DRDs is different, exhibiting peaks close to the nucleus that are almost unchanged with Z . This indicates that the mimicking of correlation in LHF and KLI is not a general feature but rather derives from systematic errors of the correction term in the inter-shell region.

To investigate further, density differences for the CO molecule were considered. Again OEPx was found to give density differences close to HF and OEP2-sc gave density differences close to those from WFT methods. However, LHF/KLI were found to have a different behaviour near the nuclei, in agreement with the analysis of the isoelectronic series and the one in Ref. 73. Accidentally, this behaviour is slightly similar to that of the conventional exchange–correlation functionals and may go some way towards explaining the observations for NMR shielding calculations in Refs. 71,72.

Finally the HOMO–LUMO gaps and HOMO energies were considered for each of the methods. The results were compared with values calculated corresponding to accurate CCSD(T) electronic densities via the approach of Ref. 48. These quantities were found to be a sensitive probe of the quality of the approaches. In general, the analysis revealed that correlation effects are quite complex for these properties, giving different trends for different systems, and that an accurate description of correlation contributions is important for accurate results. In particular, the study of the HOMO energies indicated that even at the OEP2-sc level there are evident limitations in the description of the correlation potential, so that relatively poor improvements with respect to the

OEPx results can be achieved. This could be partially connected to the finite basis set implementation of the correlated OEP procedure, in which the choice of basis set used for the calculations play a crucial role in the description of subtle correlation effects visible in HOMO energies. Nevertheless, these limitations may be thought to be mainly systematic and are thus often hidden by error cancellation effects, as in the case of HOMO–LUMO gaps.

Overall, our results show that the *ab initio* DFT OEPx and OEP2-sc approaches provide density-functional exchange and correlation energies that are similar to those in traditional wave function approaches. We have also shown that care must be taken when applying the LHF and KLI approximate exchange approaches. Whilst these approximations may be accurate in terms of their energies they can show important differences in the densities and HOMO–LUMO gaps they produce. Nevertheless it has been recently shown that LHF KS orbital energies yield very accurate TD-DFT excitation energies for a wide class of molecular systems⁶⁸. Finally, good consistency between the OEP2-sc and KS[CCSD(T)] results was observed, supporting the idea that this method can be used as a benchmark against which to test new density functional approximations. Although, a deeper analysis

of the HOMO eigenvalues from this approach indicated that some limitations exist also for this advanced method and further work will be needed to improve the description of subtle correlation effects.

Acknowledgments

It is a pleasure to dedicate this work to Prof. Rodney J. Bartlett on the occasion of his 70th birthday. We would like to thank Rod for sharing his ideas, many stimulating discussions, and for giving two of us (I.G, Sz.S) the opportunity to work together at the Quantum Theory Project.

This work was partially supported by the Polish Committee for Scientific Research MNiSW under Grant no. N N204 560839, the National Science Center under Grant No. DEC-2012/05/N/ST4/02079, and the European Research Council (ERC) Starting Grant FP7 Project DE-DOM, Grant No. 207441. A. M. T. gratefully acknowledges support via the Royal Society University Research Fellowship scheme. We thank TURBOMOLE GmbH for providing the TURBOMOLE program package and M. Margarito for technical support.

-
- ¹ W. Kohn and L. J. Sham, Phys. Rev. **140**, A1133 (1965).
² P. Hohenberg and W. Kohn, Phys. Rev. **136**, B864 (1964).
³ J. B. Krieger, Y. Li, and G. J. Iafrate, Phys. Lett. A **146**, 256 (1990).
⁴ E. Engel and S. H. Vosko, Phys. Rev. A **47**, 2800 (1993).
⁵ T. Grabo, T. Kreibich, S. Kurth, and E. K. U. Gross, in *The Strong Coulomb Correlations and Electronic Structure Calculations: Beyond Local Density Approximations*, edited by V. Anisimov (Gordon and Breach, London, 1999).
⁶ A. Görling, Phys. Rev. Lett. **83**, 5459 (1999).
⁷ S. Ivanov, S. Hirata, and R. J. Bartlett, Phys. Rev. Lett. **83**, 5455 (1999).
⁸ S. Hirata, S. Ivanov, I. Grabowski, R. J. Bartlett, K. Burke, and J. D. Talman, J. Chem. Phys. **115**, 1635 (2001).
⁹ F. Della Sala and A. Görling, J. Chem. Phys. **115**, 5718 (2001).
¹⁰ O. V. Gritsenko and E. J. Baerends, Phys. Rev. A **64**, 042506 (2001).
¹¹ F. Della Sala and A. Görling, J. Chem. Phys. **118**, 10439 (2003).
¹² V. N. Staroverov, G. E. Scuseria, and E. R. Davidson, J. Chem. Phys. **125**, 081104 (2006).
¹³ T. Heaton-Burgess, F. A. Bulat, and W. Yang, Phys. Rev. Lett. **98**, 256401 (2007).
¹⁴ A. Heßelman, A. W. Götz, F. Della Sala, and A. Görling, J. Chem. Phys. **127**, 054102 (2007).
¹⁵ A. Görling and M. Levy, Phys. Rev. A **50**, 196 (1994).
¹⁶ I. Grabowski, S. Hirata, S. Ivanov, and R. J. Bartlett, J. Chem. Phys. **116**, 4415 (2002).
¹⁷ R. J. Bartlett, I. Grabowski, S. Hirata, and S. Ivanov, J. Chem. Phys. **122**, 034104 (2005).
¹⁸ I. Grabowski and V. Lotrich, Mol. Phys. **103**, 2087 (2005).
¹⁹ P. Mori-Sánchez, Q. Wu, and W. Yang, J. Chem. Phys. **123**, 062204 (2005).
²⁰ A. Heßelman, J. Chem. Phys. **122**, 244108 (2005).
²¹ H. Jiang and E. Engel, J. Chem. Phys. **123**, 224102 (2005).
²² I. V. Schweigert, V. F. Lotrich, and R. J. Bartlett, J. Chem. Phys. **125**, 104108 (2006).
²³ D. Bokhan and R. J. Bartlett, Chem. Phys. Lett. **427**, 466 (2006).
²⁴ I. Grabowski, V. Lotrich, and R. J. Bartlett, J. Chem. Phys. **127**, 154111 (2007).
²⁵ E. Fabiano and F. Della Sala, J. Chem. Phys. **126**, 214102 (2007).
²⁶ M. Hellgren and U. von Barth, Phys. Rev. B **76**, 075107 (2007).
²⁷ I. Grabowski, Int. J. Quantum Chem. **108**, 2076 (2008).
²⁸ M. Weimer, F. Della Sala, and A. Görling, J. Chem. Phys. **128**, 144109 (2008).
²⁹ M. Hellgren and U. von Barth, J. Chem. Phys. **132**, 044101 (2010).
³⁰ P. Verma and R. J. Bartlett, J. Chem. Phys. **136**, 044105 (2012).
³¹ M. Hellgren, D. R. Rohr, and E. K. U. Gross, J. Chem. Phys. **136**, 034106 (2012).
³² P. Bleiziffer, A. Heßelman, and A. Görling, J. Chem. Phys. **139**, 084113 (2013).
³³ I. Grabowski, E. Fabiano, and F. Della Sala, Phys. Rev. B **87**, 075103 (2013).
³⁴ R. T. Sharp and G. K. Horton, Phys. Rev. **90**, 317 (1953).
³⁵ J. D. Talman and W. F. Shadwick, Phys. Rev. A **14**, 36 (1976).
³⁶ A. Görling and M. Levy, Int. J. Quantum Chem. Symp.

- 29**, 93 (1995).
- 37 S. Kümmel and L. Kronik, *Rev. Mod. Phys.* **80**, 3 (2008).
 - 38 F. Della Sala, in *Chemical Modelling, vol. 7*, edited by M. Springborg (Royal Society of Chemistry, London, UK, 2011), pp. 115–161.
 - 39 E. Engel and R. M. Dreizler, *Density Functional Theory* (Springer, Berlin, 2011).
 - 40 R. J. Bartlett, *Mol. Phys.* **108**, 3299 (2010).
 - 41 I. Grabowski, V. Lotrich, and S. Hirata, *Mol. Phys.* **108**, 3313 (2010).
 - 42 I. Grabowski, A. M. Teale, S. Śmiga, and R. J. Bartlett, *J. Chem. Phys.* **135**, 114111 (2011).
 - 43 V. Lotrich, R. J. Bartlett, and I. Grabowski, *Chem. Phys. Lett.* **405**, 33 (2005).
 - 44 K. Jankowski, K. Nowakowski, I. Grabowski, and J. Wasilewski, *J. Chem. Phys.* **130**, 164102 (2009).
 - 45 K. Jankowski, K. Nowakowski, I. Grabowski, and J. Wasilewski, *Theor. Chem. Acc.* **125**, 433 (2010).
 - 46 S. H. Vosko, L. Wilk, and M. Nusair, *Can. J. Phys.* **55**, 1200 (1980).
 - 47 C. Lee, W. Yang, and R. G. Parr, *Phys. Rev. B* **37**, 785 (1988).
 - 48 Q. Wu and W. Yang, *J. Chem. Phys.* **118**, 2498 (2003).
 - 49 L. J. Sham and M. Schlüter, *Phys. Rev. Lett.* **51**, 1888 (1983).
 - 50 R. J. Bartlett, in *Modern electronic structure theory, Part I*, edited by D. R. Yarkony (World Scientific, Singapore, 1995), pp. 1047–1131.
 - 51 S. Ivanov, S. Hirata, and R. J. Bartlett, *J. Chem. Phys.* **116**, 1269 (2002).
 - 52 D. P. Joubert, *J. Chem. Phys.* **127**, 244104 (2007).
 - 53 C. Kollmar and M. Filatov, *J. Chem. Phys.* **127**, 114104 (2007).
 - 54 M. J. G. Peach, J. A. Kattirtzi, A. M. Teale, and D. J. Tozer, *J. Chem. Phys.* **114**, 7179 (2010).
 - 55 V. N. Glushkov, S. I. Fesenko, and H. M. Polatoglou, *Theor. Chem. Acc.* **124**, 365 (2009).
 - 56 A. Theophilou and V. Glushkov, *J. Chem. Phys.* **124**, 034105 (2006).
 - 57 F. A. Bulat, T. Heaton-Burgess, A. J. Cohen, and W. Yang, *J. Chem. Phys.* **127**, 174101 (2007).
 - 58 R. Colle and R. K. Nesbet, *J. Phys. B* **34**, 2475 (2001).
 - 59 J. C. Slater, *Phys. Rev.* **81**, 385 (1951).
 - 60 F. Della Sala and A. Görling, *J. Chem. Phys.* **116**, 5374 (2002).
 - 61 A. P. Gaiduk and V. N. Staroverov, *The Journal of Chemical Physics* **128**, 204101 (pages 6) (2008), URL <http://link.aip.org/link/?JCP/128/204101/1>.
 - 62 I. G. Ryabinkin, A. A. Kananenka, and V. N. Staroverov, *Phys. Rev. Lett.* **111**, 013001 (2013), URL <http://link.aps.org/doi/10.1103/PhysRevLett.111.013001>.
 - 63 M. Weimer, F. Della Sala, and A. Görling, *Chem. Phys. Lett.* **372**, 538 (2003).
 - 64 E. Fabiano, F. Della Sala, R. Cingolani, M. Weimer, and A. Görling, *J. Phys. Chem. A* **109**, 3078 (2005).
 - 65 E. Fabiano, M. Piacenza, and F. Della Sala, *Phys. Chem. Chem. Phys.* **11**, 9160 (2009).
 - 66 E. Fabiano, M. Piacenza, S. D’Agostino, and F. Della Sala, *J. Chem. Phys.* **131**, 234101 (2009).
 - 67 F. Della Sala, E. Fabiano, S. Laricchia, S. D’Agostino, and M. Piacenza, *Int. J. Quant. Chem.* **110**, 2162 (2010).
 - 68 F. Della Sala and E. Fabiano, *Chem. Phys.* **391**, 19 (2011).
 - 69 S. Laricchia, E. Fabiano, and F. Della Sala, *Chem. Phys. Lett.* **518**, 114 (2011).
 - 70 A. Tanwar, E. Fabiano, P. E. Trevisanutto, L. Chiodo, and F. Della Sala, *Eur. Phys. J. B* **86**, 161 (2013).
 - 71 A. M. Teale and D. J. Tozer, *Chem. Phys. Lett.* **383**, 109 (2004).
 - 72 W. Hieringer, F. Della Sala, and A. Görling, *Chem. Phys. Lett.* **383**, 115 (2004).
 - 73 A. M. Teale and D. J. Tozer, *Phys. Chem. Chem. Phys.* **7**, 2991 (2005).
 - 74 ACES II (Quantum Theory Project, University of Florida); written by; J. S. Stanton, J. Gauss, J. D. Watts, M. Nooijen, N. Oliphant, S. A. Perera, P. G. Szalay, W. J. Lauderdale, S. A. Kucharski, S. R. Gwaltney, S. Beck, A. Balkov, D. E. Bernholdt, K. K. Baeck, P. Rozyczko, H. Sekino, C. Hober and R. J. Bartlett. Containing contributions from VMOL (J. Almlöf and P. R. Taylor); VPROPS (P. Taylor); ABACUS; (T. Helgaker, H. J. Aa. Jensen, P. Jørgensen, J. Olsen, and P. R. Taylor) (2007).
 - 75 *TURBOMOLE V6.4 2012, a development of University of Karlsruhe and Forschungszentrum Karlsruhe GmbH, 1989-2007, TURBOMOLE GmbH, since 2007; available from <http://www.turbomole.com>.*
 - 76 *Dalton, a molecular electronic structure program, release 2.0 (2005), see <http://www.kjemi.uio.no/software/dalton/dalton.html>.*
 - 77 N. C. Handy and H. F. Schaefer III, *J. Chem. Phys.* **81**, 5031 (1984).
 - 78 J. E. Rice and R. D. Amos, *Chem. Phys. Lett.* **122**, 585 (1985).
 - 79 R. J. Bartlett, in *Geometrical Derivatives of Energy Surfaces and Molecular Properties*, edited by P. Jørgensen and J. Simons (Reidel, Dordrecht, The Netherlands, 1986), pp. 35–61.
 - 80 E. A. Salter, G. W. Trucks, and R. J. Bartlett, *J. Chem. Phys.* **90**, 1752 (1989).
 - 81 T. Helgaker and P. Jørgensen, *Theor. Chim. Acta* **75**, 111 (1989).
 - 82 P. Jørgensen and T. Helgaker, *J. Chem. Phys.* **89**, 1560 (1988).
 - 83 H. Koch, H. J. A. Jensen, P. Jørgensen, T. Helgaker, G. E. Scuseria, and H. F. Schaefer III, *J. Chem. Phys.* **92**, 4924 (1990).
 - 84 K. Hald, A. Halkier, P. Jørgensen, S. Coriani, C. Hättig, and T. Helgaker, *J. Chem. Phys.* **118**, 2985 (2003).
 - 85 P. O. Widmark, P. A. Malmqvist, and B. Roos, *Theor. Chim. Acta* **77**, 291 (1990).
 - 86 K. A. Peterson and T. H. Dunning, Jr., *J. Chem. Phys.* **117**, 10548 (2002).
 - 87 T. H. Dunning, Jr., *J. Chem. Phys.* **90**, 1007 (1989).
 - 88 E. R. Davidson, H. A. Hagstrom, S. J. Chakravorty, V. M. Umar, and C. F. Fischer, *Phys. Rev. A* **52**, 7071 (1991).
 - 89 B. Verstichel, H. van Agglen, D. van Neck, P. W. Ayers, and P. Bultinck, *Phys. Rev. A* **80**, 032508 (2009).
 - 90 J. C. Slater, *Quantum Theory of Molecules and Solids*, vol. 4: The Self-Consistent Field for Molecules and Solids (McGraw-Hill, New York, 1974).
 - 91 A. Becke, *Phys. Rev. A* **38**, 3098 (1988).
 - 92 M. Petersilka, E. K. U. Gross, and K. Burke, *Int. J. Quantum Chem.* **80**, 534 (2000).
 - 93 R. J. Magyar, A. Fleszar, and E. K. U. Gross, *Phys. Rev. A* **69**, 045111 (2004).
 - 94 P. J. Wilson and D. J. Tozer, *J. Chem. Phys.* **116**, 10139 (2002).
 - 95 A. Radzig and B. Smirnov, *Reference data on atoms and*

molecules (Springer, Berlin, 1985).

⁹⁶ T. Grabo and E. K. U. Gross, Chem. Phys. Lett. **240**, 141 (1995).

⁹⁷ <http://webbook.nist.gov>.